International Journal of Cardiology 283 (2019) 9–16

Contents lists available at ScienceDirect

International Journal of Cardiology

journal homepage: www.elsevier.com/locate/ijcard

Secretory vimentin is associated with coronary artery disease in patients and induces atherogenesis in *ApoE*$^{-/-}$ mice

Dong Huo Gong [a,b,1], Yang Dai [a,b,1], Shuai Chen [b], Xiao Qun Wang [a], Xiao Xiang Yan [a], Ying Shen [a], Jing Liu [b], Zhen Kun Yang [a], Jian Hu [a], Lin Jun Yu [a], Li Li Liu [a], Rui Yan Zhang [a], Wei Feng Shen [a], Qiu Jing Chen [b], Feng Hua Ding [a,*], Lin Lu [a,b,*]

[a] Department of Cardiology, Rui Jin Hospital, Shanghai Jiaotong University School of Medicine, Shanghai, People's Republic of China
[b] Institute of Cardiovascular Diseases, Shanghai Jiaotong University School of Medicine, Shanghai, People's Republic of China

ARTICLE INFO

Article history:
Received 6 December 2018
Received in revised form 25 January 2019
Accepted 15 February 2019
Available online 16 February 2019

Keywords:
Secretory vimentin
Coronary artery disease
Atherogenesis

ABSTRACT

Purpose: The present study aimed to investigate the relationship between serum levels of secretory vimentin and coronary artery disease (CAD). The biological effect of secretory vimentin was ascertained by experiments.
Methods: We analysed serum levels of secretory vimentin in CAD patients (n = 288) and non-CAD controls (n = 195) by ELISA. To evaluate the pro-inflammatory effects of secreted vimentin, the human aortic endothelial cells (HAECs) and human peripheral blood mononuclear cells (PBMCs) were treated with recombinant vimentin or saline. Intraperitoneal injection of vimentin (1 μg/each) or saline was performed every other day for 12 weeks in *ApoE*$^{-/-}$ mice for assessment of atherogenic effect.
Results: Serum levels of secretory vimentin were significantly increased in CAD patients than in health controls ($p < 0.05$), and correlated with the number of diseased coronary arteries, Syntax and Gensini score (for all comparison, $p < 0.01$). Logistic regression analysis showed that vimentin level is an independent determinant of CAD. In experiments, recombinant vimentin protein enhanced the expression of adhesion molecules and inflammatory cytokines in both endothelial cells and macrophages. This protein also promoted macrophage-endothelial cells adhesion *in vitro* and the recruitment of leukocytes to mesenteric venules in C57BL/6 mice. Compared with saline, intraperitoneal injection of recombinant vimentin (1 μg/each) every other day induced atherogenesis in *ApoE*$^{-/-}$ mice at 12-weeks, with significant increase of inflammatory cytokine and adhesion molecules expression in aortic tissue ($p < 0.05$).
Conclusion: Serum vimentin levels are associated with the presence and the severity of CAD. Vimentin protein promotes atherogenesis in *ApoE*$^{-/-}$ mice.

1. Introduction

Vascular inflammatory reactions involving endothelial cells and activated macrophages promote atherogenesis [1]. Accumulating evidence has revealed that vimentin, a type III intermediate filament that regulates dynamic cellular processes such as cell adhesion and migration, is closely related to inflammation [2]. For instance, the interaction between vimentin and the NLRP3 inflammasome results in NLRP3 activation, which is crucial for the pro-inflammatory effects of macrophage migration inhibitory factors [3]. Compared with wild-type mice, vimentin-deficient mice exhibit attenuated pathogenic features in lung tissue after lipopolysaccharide (LPS) challenge, as represented by reductions in inflammation, IL-1β levels and endothelial permeability [4]. Vimentin in endothelial cells and lymphocytes functions to form anchoring structures between these two cell types, contributing to the adhesion and transmigration of lymphocytes [5]. Moreover, vimentin binds the promoter of 12/15-lipoxygenase to modulate its expression and activity [6], and 12/15-lipoxygenase plays a dominant role in the development of atherosclerosis by promoting endothelial inflammation and foam cell formation [7].

It is noteworthy that vimentin is secreted from a distinct population of vascular endothelial cells and activated macrophages, with significant accumulation in circulating human blood [8,9]. PAL-E (anti-vimentin antibody)-reactive circulatory vimentin does not arise from an endothelial cell-specific mRNA transcript but rather is the product of cell-specific posttranslational phosphorylation modification [8,9]. The anti-inflammatory cytokine IL-10 blocks the secretion of vimentin, whereas the pro-inflammatory cytokine TNF-α triggers its secretion, suggesting the involvement of secretory vimentin in inflammation. However, the biological role of secretory vimentin is currently unknown.

* Corresponding authors at: Department of Cardiology, Rui Jin Hospital, 197 Rui Jin Road II, Shanghai 200025, PR China.
E-mail addresses: dfh11114@rjh.com.cn (F.H. Ding), rjlulin1965@163.com (L. Lu).
[1] These authors contributed equally in this study.

https://doi.org/10.1016/j.ijcard.2019.02.032

The present study aimed to investigate the relationship between secretory vimentin and atherosclerosis. Thus, we evaluated serum levels of secretory vimentin in patients with coronary artery disease (CAD) and healthy control subjects. To test the biological influence of secretory vimentin, we treated endothelial cells and macrophages with recombinant vimentin and subsequently evaluated any pro-inflammatory effects. This protein was also injected intraperitoneally into *ApoE*$^{-/-}$ mice to assess atherogenesis. To the best of our knowledge, our study is the first to probe the effects of secretory vimentin.

2. Methods and materials

2.1. Study population

Declaration of Helsinki: The present study complied with the Declaration of Helsinki. The study protocol was approved by the local hospital ethics committee, and written informed consent was obtained from all subjects.

This study included 288 consecutive patients with stable angina or stable asymptomatic CAD who underwent coronary angiography examination or interventional treatment from November 2016 to March 2017 in the Department of Cardiology, Rui Jin Hospital, Shanghai Jiaotong University School of Medicine. Significant CAD was diagnosed if luminal diameter narrowing ≥70% was present at a major epicardial coronary artery, and left main coronary artery narrowing ≥50% was considered a 2-vessel disease. Patients with CAD were further classified according to the number of diseased coronary arteries (1-, 2-, or 3-vessel disease). For study purposes, patients with concomitant vascular heart disease, congenital heart disease, acute coronary syndromes, previous myocardial infarction, congestive heart failure, or a history of stroke, malignancy, connective tissue diseases, acute/chronic infection, or severe renal insufficiency were excluded.

Another 195 subjects with no evidence or history of vascular disease served as controls. These subjects were from outpatient clinics around our hospital and received an annual physical check-up. They had a normal resting electrocardiogram and exercise stress test, as well as normal carotid artery ultrasound examination and echocardiography. None had any evidence of cardiovascular disease (including exclusion of any previous history of angina/myocardial infarction). All subjects underwent serum biochemical measurements, including lipid profile, liver and kidney function tests and hsCRP.

2.2. Coronary angiography and analysis

Coronary angiography was performed using a radial or femoral approach [10]. Quantitative coronary angiography (QCA) was performed by two interventional cardiologists using Cardiovascular Measurement System version 3.0 software (Terra, GE, USA) who were blinded to the study protocol. Significant CAD was diagnosed if luminal diameter narrowing was estimated as ≥70% in a major epicardial coronary artery. Left main coronary artery stenosis ≥50% was considered a 2-vessel disease. The total Syntax score was composed of the individual scores for each separate lesion with diameter stenosis ≥50% in a vessel ≥1.5 mm in diameter by visual assessment [10]. The Gensini score was calculated according to the method presented by Gensini [11].

2.3. Determination of serum secretory vimentin levels by ELISA

Serum levels of secretory vimentin in study participants were determined using ELISA. ELISA kits for secretory vimentin were obtained from Lifespan Biosciences (Seattle, WA). The range reference of ELISA kit is 7.83-500 ng/mL.

2.4. Antibodies

All chemicals were obtained from Sigma Aldrich (St. Louis, MO). Rabbit anti-VCAM-1 and rabbit anti-ICAM-1 antibodies were purchased from Cell Signaling Technology (Beverly, MA). Rabbit anti-TNF-α, rabbit anti-IL6, rabbit anti-IL1β, rabbit anti-CCR2 and rabbit anti-MOMA-2 antibodies were purchased from Abcam (Cambridge, UK). Antibodies targeting tubulin and α-SMA were purchased from Santa Cruz Biotechnology (Santa Cruz, CA).

2.5. Animal experiments and quantification of atherosclerotic lesions

All animal experiments were conducted in compliance with the Guide for the Care and Use of Laboratory Animals by the US National Institutes of Health (NIH Publication No. 85-23, revised 1996) and approved by the Hospital Animal Care Committee.

In-house bred C57BL/6 and *ApoE*$^{-/-}$ mice were housed in a pathogen-free environment at the Animal Experiment Centre of Rui Jin Hospital, Shanghai Jiaotong University School of Medicine. The animals were allowed access to food and water *ad libitum* on a 12-hour light/dark cycle. *ApoE*$^{-/-}$ mice were initially fed a standard rodent chow diet until 8 weeks of age and then switched to either a high-fat diet (D12109C) or a control diet obtained from Research Diets Inc. (New Brunswick, NJ).

Male C57BL/6 and *ApoE*$^{-/-}$ mice (8–10 weeks) received an intraperitoneal injection of PBS or vimentin (1 μg/injection) every other day for 12 weeks. Plasma was separated by centrifugation and stored at −80 °C. The lipid profiles, including total cholesterol, high-density lipoprotein-cholesterol (HDL-C), low-density lipoprotein-cholesterol (LDL-C), and triglyceride concentrations, were determined by standard enzymatic colorimetric techniques (#Modular-P800, Roche Diagnostics, Laval, Quebec) according to the manufacturer's procedures.

After completion of the experiments, aortas were isolated from animal models, and the atherosclerotic lesion size was quantified using computerized image analysis after staining the entire aorta with Oil red O. The percentage of lesion coverage was calculated by dividing the stained area by the total thoraco-abdominal aortic surface. The expression levels of adhesion molecules and other inflammatory factors in the aorta were analysed by western blot. The plasma levels of MCP1, IL-6, IL-1β and TNF-α were determined with commercial ELISA kits from Abcam plc. (Cambridge, UK).

2.6. Preparation of recombinant vimentin protein

Expression of human vimentin was induced in BL21 cells by 1 mM IPTG, and the protein was isolated by binding to Ni-agarose beads and eluted with imidazole. Next, the extracted vimentin protein was purified by reverse-phase HPLC using a SOURCE 15 RPC column (GE Healthcare, Uppsada, Sweden), and endotoxin was removed by using a ToxOut™ Rapid Endotoxin Removal Kit (Biovision, CA.). Purified fractions were analysed by SDS/PAGE and western blot and then lyophilized. To exclude the effect of LPS, we detected TLR4 and MyD88 expression in human aortic endothelial cells (HAECs) treated with recombinant vimentin and observed the expression of inflammatory and adhesion factors in HAECs treated with native vimentin or denatured vimentin.

2.7. Cell culture

HAECs were purchased from ScienCell Research Laboratories (San Diego, CA) and grown in Endothelial Cell Medium and cultured at 37 °C in a humidified atmosphere containing 5% CO2. THP-1 monocytoid cell lines were purchased from American Type Culture Collection (ATCC, Manassas, VA, USA) and cultured in RPMI 1640 medium as described above [12].

2.8. Isolation of human peripheral blood monocytes

We isolated peripheral blood mononuclear cells (PBMCs) in peripheral blood from healthy volunteers using dextran sedimentation and Ficoll-Hypaque density-gradient separation as previously described [12]. We lysed purified PBMCs in lysis buffer containing 20 mM TRIS (pH 7.4), 150 mM NaCl, 1 mM EDTA, 1 mM EGTA, 1% Triton, 0.1% SDS and a protease inhibitor cocktail and stored the lysates at −80 °C until use. Moreover, peripheral blood monocytes were enriched from PBMCs by negative selection using a magnetically negative depletion protocol (Miltenyi Biotec) [12]. Then, PBMCs were used for cell experiments.

2.9. Intravital microscopy

Intravital microscopy of leukocyte-endothelium interactions was performed as previously described [12]. Mice were anaesthetized with sodium pentobarbital 4 h after receiving a bolus of PBS or vimentin (10 μg). Leukocytes were labelled by retro-orbital injection of 50 μL of 0.05% Rhodamine 6G. We then exteriorized the mesenteric venules and kept the system at 37 °C on a stage warmer. The rolling leukocytes were monitored in real time with an inverted fluorescence microscope (IX71, Olympus). The leukocyte rolling velocity and the number of rolling and adherent leukocytes were analysed with NIH Image-Pro Plus v 6.2 software (Media Cybernetics, Bethesda, MD) [12]. We defined leukocytes attached to the vessel wall for >5 s as adherent cells.

2.10. In vitro THP-1 monocyte adhesion assay

An endothelial cell adhesion assay was performed using a commercially available kit (ECM645, Millipore) [13]. Briefly, HAECs were seeded in black clear-bottom tissue culture plates and grown for 48 to 72 h or until confluent. The cells were treated with the control pro-inflammatory factor TNF-α, and then Calcein-AM-labelled THP-1 cells were added to the wells. The plate was incubated briefly to allow cell binding, while non-specific cells were washed off. Finally, the plate was read at 485 nm excitation/530 nm emission in a fluorescent plate reader.

2.11. Western blot analysis

The cells were harvested and lysed in lysis buffer containing protease inhibitor cocktail. Protein concentrations were determined by the Bradford protein assay and cell lysates were subjected to SDS-polyacrylamide gel electrophoresis. The proteins were transferred to nitrocellulose membranes, after which they were blocked in blocking buffer. Then, the blots were incubated overnight at 4 °C with appropriate primary antibodies followed by incubation with HRP-conjugated secondary antibodies after washing. Images were acquired using an Odyssey Infrared Imaging System (Li-Cor Biosciences, Lincoln, NE). Densitometric analysis of protein bands was performed using ImageJ software (version 1.36b, National Institutes of Health).

Table 1
Baseline characteristics in patients with and without CAD.

	No-CAD (n = 195)	CAD (n = 288)	*p* value
Male, n (%)	99 (50.8)	210 (72.9)	<0.001
Age, year	62.29 ± 10.03	68.11 ± 9.74	<0.001
Body mass index, Kg/m^2	24.76 ± 3.34	24.95 ± 3.31	0.535
Hypertension, n (%)	86 (44.1)	207 (71.9)	<0.001
Diabetes, n (%)	27 (13.8)	100 (34.7)	<0.001
Smoking, n (%)	44 (22.6)	133 (46.2)	<0.001
Systolic blood pressure, mm Hg	132.8 ± 18.1	139.2 ± 20.8	<0.001
Diastolic blood pressure, mm Hg	76.2 ± 10.8	75.2 ± 12.2	0.330
Fasting blood glucose, mmol/L	5.76 ± 1.39	6.45 ± 2.21	<0.001
HbA1c, %	5.81 ± 0.65	6.39 ± 1.35	<0.001
Triglyceride, mmol/L	1.49 ± 0.92	1.61 ± 0.89	0.141
Total cholesterol, mmol/L	4.2 ± 1.01	4.11 ± 1.15	0.386
HDL-C, mmol/L	1.25 ± 0.30	1.16 ± 0.26	0.001
LDL-C, mmol/L	2.43 ± 0.79	2.4 ± 0.93	0.750
Serum creatine, μmol/L	76.58 ± 18.6	88.86 ± 25.14	<0.001
eGFR, mL/min/1.73 m^2	84.38 ± 15.69	74.52 ± 17.84	<0.001
Uric acid, μmol/L	334.47 ± 99.4	343.68 ± 96.42	0.310
hsCRP, mg/L	0.61 (0.35–1.43)	1.14 (0.60–3.53)	<0.001
LVEF, %	68.14 ± 9.98	63.44 ± 9.31	<0.001
Severity of CAD, n (%)			
1-vessel	/	86 (29.9)	/
2-vessel	/	98 (34.0)	/
3-vessel	/	104 (36.1)	/
Syntax score	/	15 (8–23)	/
Gensini score	0 (0–1)	25 (10–46)	<0.001
Vimentin, ng/mL	97.8 (78.1–125.5)	126.4 (97.1–172.3)	<0.001
Medication, n (%)			
Antiplatelet therapy	60 (30.8)	110 (38.2)	0.094
ACE inhibitors/ARB	101 (51.8)	181 (62.8)	0.016
β blockers	69 (35.4)	121 (42.0)	0.143
Calcium channel blockers	52 (26.7)	94 (32.6)	0.161
Statins	76 (39.0)	120 (41.7)	0.554

Data are mean ± SD or median (25th–75th percentiles) or number (%).
ACE, angiotensin converting enzyme; ARB, angiotensin receptor blocker; CAD, coronary artery disease; GFR, glomerular filtration rate; HbA1c, glycosylated hemoglobin A1c; HDL, high-density lipoprotein; hsCRP, high-sensitivity C reactive protein; LDL, low-density lipoprotein; LVEF, left ventricular ejection fraction.

3. Statistical analysis

Continuous variables are presented as the means and standard deviation (SD), and categorical data are summarized as frequencies or percentages. For continuous variables, we evaluated the existence of a normal distribution with the Kolmogorov–Smirnov test. We analysed differences among patient groups by one-way analysis of variance (ANOVA). We determined correlations between variables by the Pearson or Spearman correlation tests, as appropriate. We performed stepwise multivariable logistic regression analysis to detect the additional predicting value of secretory vimentin on the diagnosis of CAD by adopting two models. In Model 1, we included traditional risk factors of CAD (hypertension, diabetes, dyslipidemia and smoking, *etc.*) and those parameters significantly different between CAD and non-CAD control groups in Table 1. In Model 2, we additionally adjusted the analysis for secretory vimentin. Receiver operator characteristic (ROC) analysis of CAD risk factors and biohumoral measurements was performed with and without the addition of the secretory vimentin parameter. We used the C statistic to analyse the discriminatory capacity of Models 1 and 2 and performed risk reclassification using the method described by Pencina et al. [14]. We also determined the net reclassification improvement (NRI) and integrated discrimination improvement (IDI) accordingly [14,15]. For cell experiments, the data represent the average results from 3 experiments, and we performed one-way ANOVA and *t*-test analysis to assess the significance of changes relative to the controls. For animal experiments, we performed *t*-test analysis to assess the significance of changes relative to the controls. All analyses used 2-sided tests with an overall significance level alpha = 0.05, and all tests were performed with SPSS 19.0 for Windows (SPSS, Inc., Chicago, IL, USA).

4. Results

4.1. Increased serum levels of secretory vimentin are associated with the presence and severity of CAD in patients

The baseline characteristics and parameters of both CAD patients and control subjects are detailed in Table 1. The CAD group had more males, more smokers, more elderly individuals, a higher percentage of individuals with hypertension and type 2 diabetes mellitus, and lower HDL-C levels than the control group.

Notably, serum levels of secretory vimentin were significantly higher in CAD patients than in control subjects ($p < 0.001$, Table 1). We categorized CAD patients into one-vessel, two-vessel and three-vessel disease subgroups. There was a significant increase in vimentin levels across the three subgroups (122.9 ± 50.6, 135.0 ± 47.4, and 183.1 ± 117.1 ng/mL for the one-vessel, two-vessel and three-vessel subgroups, respectively; $p < 0.001$) (Fig. 1). We further stratified CAD patients into tertiles according to secretory vimentin level. These tertiles were found to be correlated significantly with Syntax and Gensini score (both $p < 0.001$) (Fig. 1).

4.2. The serum level of secretory vimentin is an independent determinant of CAD

To assess independent determinants of CAD, we performed multivariable analyses with the traditional cardiovascular risk factors and parameters detailed in Table 1. In Model 1, male gender, age, smoking, hypertension, diabetes, eGFR, hsCRP and left ventricular ejection

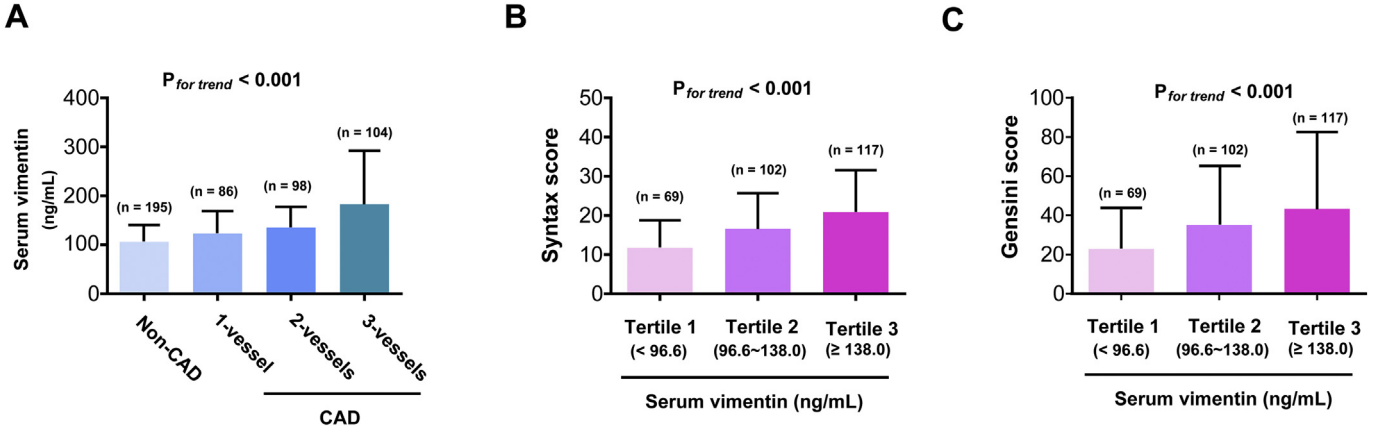

Fig. 1. Increased serum levels of secretory vimentin are associated with the presence and severity of CAD in patients.

fraction were independent determinants of CAD. When we included vimentin in the multivariable analysis in Model 2, vimentin levels remained independently associated with CAD in addition to the other conventional factors included in Model 1 (Table 2). The addition of vimentin marginally improved risk prediction (C statistics, from 0.799 to 0.822, $p = 0.010$, Supplemental Fig. 1) with an NRI of 6.6% ($p = 0.026$) and IDI of 4.2% ($p < 0.001$). The calibration of Models 1 (0.316) and 2 (0.753) was good. Inclusion of vimentin resulted in a significant 4.7% improvement (Nagelkerke R square of Model 1 [0.338] and Model 2 [0.385], $p < 0.001$) in explaining the variation in the dependent variable.

4.3. Vimentin protein promotes inflammatory reactions in endothelial cells and macrophages (PBMCs) and induces macrophage-endothelial cell adhesion in vitro

To investigate the effects of secretory vimentin on HAECs and PBMCs, we prepared recombinant vimentin and treated the cells with this protein. For these cell experiments, we chose concentrations of vimentin based on serum levels. After overnight stimulation with vimentin, the protein levels of adhesion molecules (VCAM-1 and ICAM-1) and inflammatory cytokines (IL-6 and TNF-α) were significantly increased in a concentration-dependent manner in HAECs (Fig. 2A,B). Likewise, enhanced production of IL-1β, TNF-α, CCR2 and MCP-1 was induced by vimentin in human monocytes (Fig. 2C,D). However, denatured vimentin did not show any of the abovementioned cellular effects, indicating that these effects were not due to endotoxin contamination in the vimentin preparation (Supplemental Fig. 2).

For the *in vitro* monocytoid cell-endothelium adhesion assay, HAECs were treated with vimentin at increasing concentrations (0, 1, 5, 25, and 125 ng/mL), with PBS and TNF-α serving as a negative control and positive control, respectively; the HAECs were then cocultured with THP-1 monocytoid cells. We observed a significant concentration-dependent enhancement of THP-1 monocytoid cell adhesion to endothelial cells ($p < 0.001$), a phenomenon remarkably blocked by monoclonal antibodies against VCAM-1 and ICAM-1 (Fig. 2E,F).

Table 2
Multivariable logistic regression analyses for coronary artery disease with and without vimentin.

	Variables	OR (95% CI)	*p* value
Model 1	Gender	1.669 (1.018–2.736)	0.042
	Age	1.038 (1.011–1.067)	0.006
	Body mass index	0.985 (0.921–1.053)	0.650
	Smoking	2.178 (1.272–3.730)	0.005
	Hypertension	1.820 (1.166–2.840)	0.008
	Diabetes	2.482 (1.452–4.242)	0.001
	Total-to-HDL cholesterol ratio	1.174 (0.967–1.427)	0.105
	eGFR	0.981 (0.965–0.996)	0.016
	Log-transferred hsCRP	1.262 (1.042–1.528)	0.017
	Left ventricular ejection fraction	0.963 (0.940–0.988)	0.003
Model 2	Gender	1.826 (1.092–3.054)	0.022
	Age	1.039 (1.011–1.068)	0.007
	Body mass index	0.975 (0.910–1.045)	0.468
	Smoking	2.034 (1.168–3.544)	0.012
	Hypertension	1.661 (1.050–2.628)	0.030
	Diabetes	2.331 (1.353–4.016)	0.002
	Total-to-HDL cholesterol ratio	1.206 (0.987–1.474)	0.067
	eGFR	0.978 (0.962–0.994)	0.008
	Log-transferred hsCRP	1.287 (1.056–1.569)	0.012
	Left ventricular ejection fraction	0.968 (0.944–0.993)	0.011
	Tertiles of vimentin		<0.001
	Tertile 1	1 (ref)	/
	Tertile 2	2.331 (1.393–3.901)	0.001
	Tertile 3	3.752 (2.129–6.613)	<0.001

eGFR, estimated glomerular filtration rate; HDL, high-density lipoprotein; hsCRP, high-sensitivity C reactive protein.

4.4. Vimentin induces inflammatory reactions in C57BL/6 mice and leukocyte-endothelium interactions in vivo

To evaluate the effect of vimentin *in vivo*, we intraperitoneally injected vimentin protein (1 μg/injection) or PBS every other day into C57BL/6 mice. After 12 weeks, the mice were sacrificed, and the levels of adhesion molecules and inflammatory cytokines in aortic tissue and plasma were determined. The expression levels of ICAM-1, VCAM-1, IL-6 and TNF-α were significantly increased in mice injected with vimentin compared with those in mice injected with PBS (for all comparisons, $p < 0.05$) (Fig. 3A,B). Likewise, the plasma levels of IL-1β, IL-6 MCP-1 and TNF-α were concomitantly elevated after vimentin administration (for all comparisons, $p < 0.05$) (Fig. 3C). It is also worth noting that the plasma levels of circulatory vimentin were consistent with those in human samples (data not shown).

We performed intravital microscopy to evaluate the effects of vimentin on the number of rolling leukocytes and adherent leukocytes as well as the leukocyte rolling velocity in mesenteric venules of C57BL/6 mice. Compared with PBS, vimentin induced a significant increase in adherent leukocytes and rolling leukocytes in the venules as well as an obvious reduction in their rolling velocity (Fig. 3D,E). Moreover, vimentin-induced leukocyte adhesion reflected by these measurements was profoundly attenuated by treatment with monoclonal antibodies against VCAM-1 and ICAM-1 ($p < 0.05$).

4.5. Intraperitoneal injection of vimentin promotes atherogenesis in $ApoE^{-/-}$ mice

To test whether vimentin exerts an atherogenic effect *in vivo*, we intraperitoneally injected recombinant vimentin protein (1 μg/injection) (vimentin group, n = 12) or saline (saline group, n = 12) every other day into $ApoE^{-/-}$ mice fed high-fat chow. Mice from both groups were then sacrificed at 12 weeks. During this experiment, 1 mouse in the vimentin group died of peritoneal infection. After 12 weeks, mice treated with vimentin showed significantly increased atherosclerotic lesion area throughout the entire aorta and in the aortic root compared with that in saline-treated mice ($p < 0.05$) (Fig. 4), although there was no significant difference in the serum profiles (including triglyceride, LDL-C, total cholesterol, and HDL-C) between two groups (Supplemental Fig. 4).

5. Discussion

The present study has demonstrated that increased serum levels of secretory vimentin are associated with the presence and severity of CAD, and the vimentin level is an independent determinant of CAD. Vimentin protein promotes inflammatory reactions in both *in vitro* endothelial cell and macrophage experiments and mice. Intraperitoneal injection of vimentin induces atherogenesis in $ApoE^{-/-}$ mice fed a high-fat diet. Jointly, these results suggest that secretory vimentin causes atherosclerosis in CAD patients.

Intermediate filament proteins are classified into several groups according to their molecular structure. Vimentin is one of the most widely expressed type III intermediate filament proteins. It is the only cytoplasmic intermediate filament found in lymphocytes, neutrophils, endothelial cells, fibroblasts and macrophages [16,17]. Vimentin has been shown to act as a scaffold for signaling proteins that regulate cancer cell invasion [18], wound healing and tissue repair [19], tissue ageing [20], and apoptosis [16,17]. Vimentin also facilitates the inflammatory response by regulating activation of the NLRP3 inflammasome [21] and anchors and organizes adhesion molecules as well as actomyosin complexes to regulate cell adhesion and migration [22]. In addition, increased levels of vimentin have been observed in atherosclerotic lesions and have been suggested to be linked to endothelial-to-mesenchymal transition (EndMT) [23].

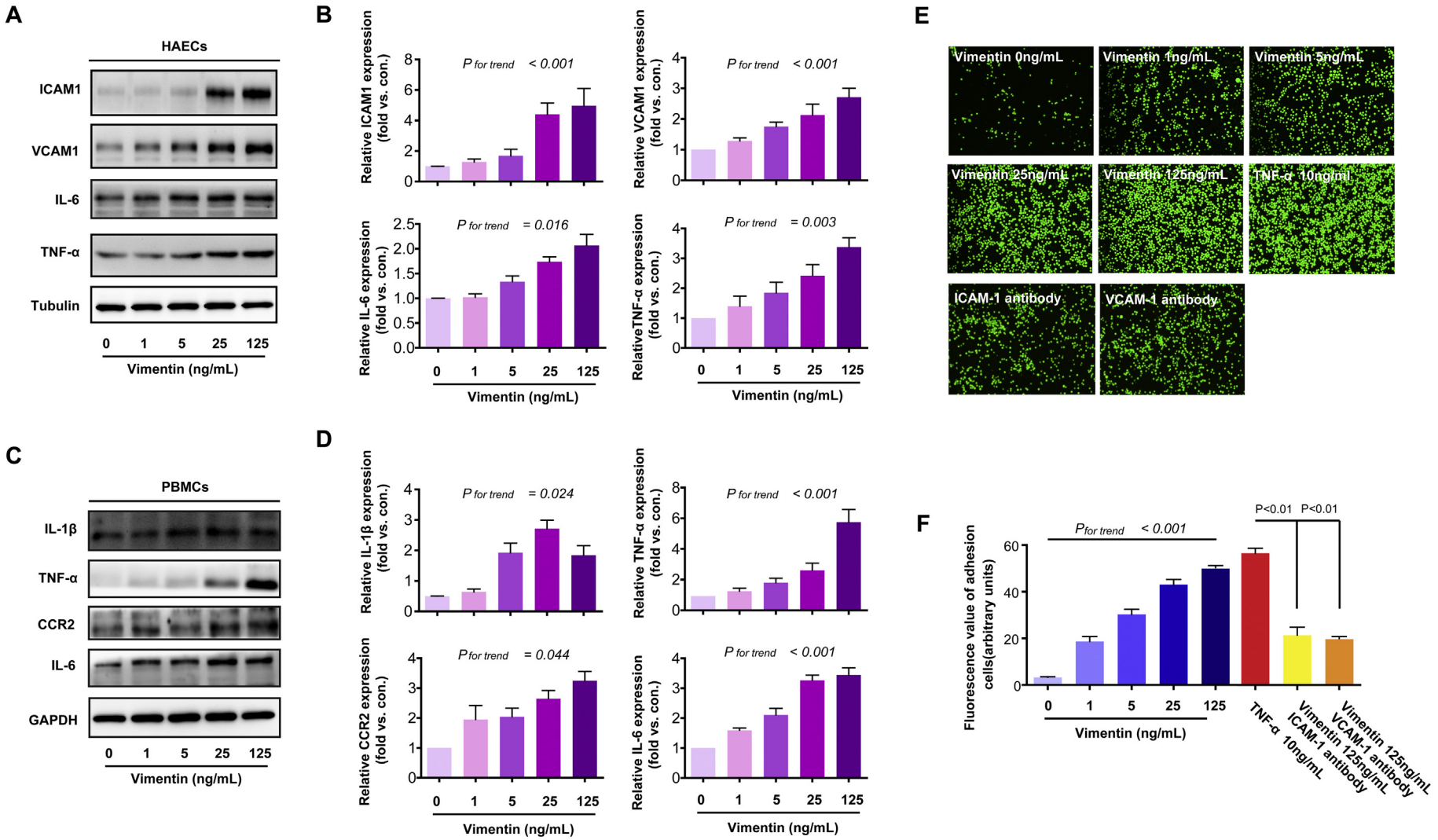

Fig. 2. Vimentin upregulates the protein levels of adhesion molecules and inflammatory cytokines in endothelial cells and macrophages and induces macrophage-endothelial cell adhesion *in vitro*. HAECs were stimulated with increasing concentrations of recombinant vimentin protein (0, 1, 5, 25, 125 ng/mL) overnight, and the expression of adhesion molecules and inflammatory cytokines was determined by western blot analysis (A). Quantification of data in experiment A (B). Human peripheral blood mononuclear cells (PBMCs) were stimulated with increasing concentrations of recombinant vimentin (0, 1, 5, 25, 125 ng/mL) overnight. The expression of inflammatory cytokines was determined by western blot analysis (C). Quantification of data in experiment C (D). HAECs were stimulated with PBS, TNF-α (10 ng/mL, as a positive control) or vimentin (0–125 ng/mL) for 16 h. Monocytoid THP-1 cells were labelled with 2′7′-bis-(2-carboxyethyl)-5-(and-6)-carboxyfluorescein-acetoxymethylester (BCECF-AM) and then coincubated with HAECs for 30 min (E). Quantification of adherent THP-1 cells to HAECs per square millimetre surface area by fluorescence quantitative analysis (F). Values are expressed as the mean ± SD. Statistical analyses were performed using one-way ANOVA and *t*-test.

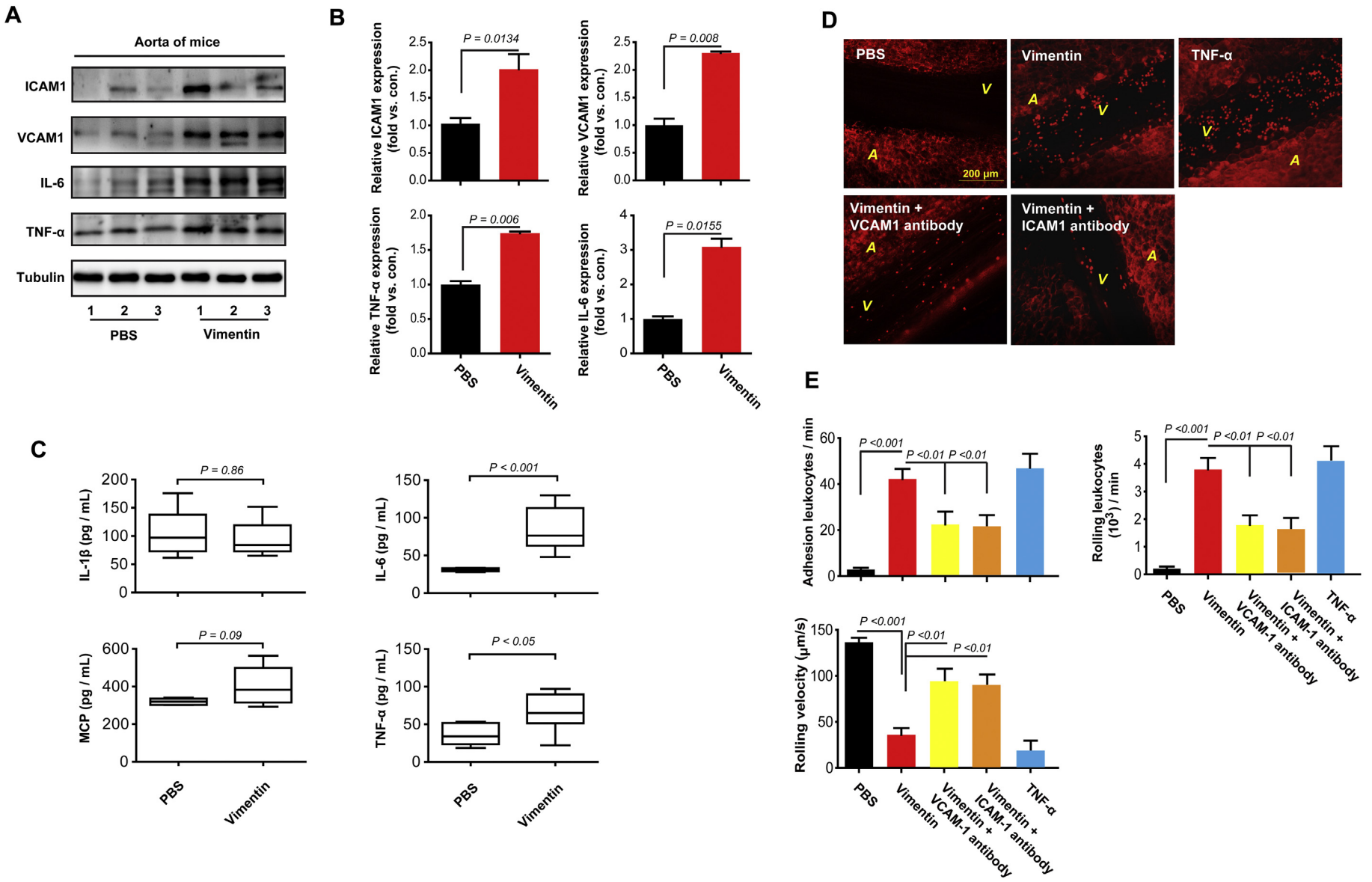

Fig. 3. Vimentin increases the expression of adhesion molecules and inflammatory cytokines and induces the adhesion of macrophages to endothelial cells *in vivo*. Intraperitoneal injections of PBS or vimentin (1 μg/injection) into C57BL/6 mice (n = 10/each group) were performed every other day for 3 months. Adhesion molecule and cytokine levels in the aortic tissues of the animal models were determined by western blotting (A). The quantitative results are shown in (B). Serum inflammatory factors, including TNF-α, IL-6, MCP-1 and IL-1β, were measured by ELISA (C). Representative images of rolling leukocytes within the mesenteric venules from C57BL/6 mice 4 h after intraperitoneal injection of PBS or vimentin (10 μg/injection) (D). 'A' indicates adipose tissue of the vessel wall, and 'V' indicates the lumen of the venules. Bright red dots in the venules represent rhodamine-labelled rolling leukocytes. Leukocyte rolling flux was processed by Image-Pro into a simplified form for the automatic recognition and tracking of rolling leukocytes. The adhesive leukocyte number, rolling time and rolling velocity were quantified (E). Values are expressed as the mean ± SD. Statistical analyses were performed using a *t*-test.

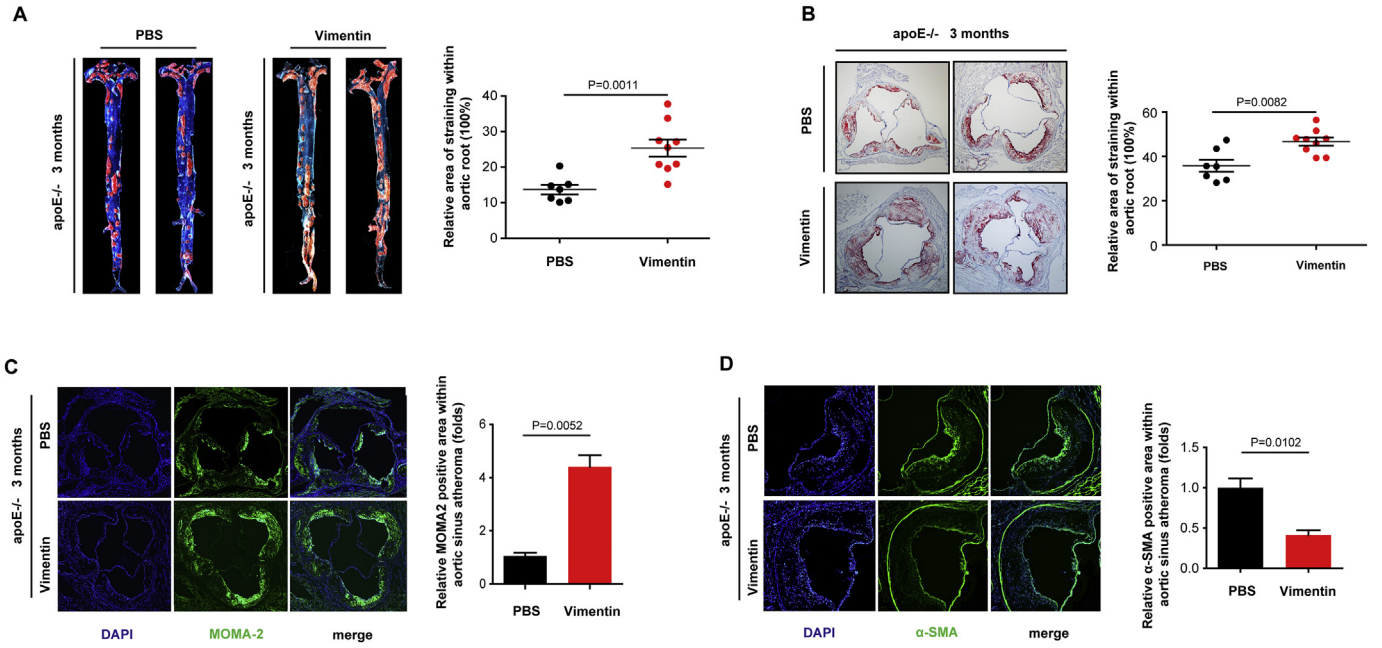

Fig. 4. Intraperitoneal injection of vimentin promotes atherogenesis and alters lesion composition in *ApoE*$^{-/-}$ mice. PBS or vimentin (1 μg/injection) was intraperitoneally injected into male *ApoE*$^{-/-}$ mice (n = 12/each group) every other day. After the mice were fed a high-cholesterol diet for 12 weeks, they were euthanized, and their aortas were isolated. The atherosclerotic lesion area in the aortas and aortic roots were stained with Oil red O (A) and (C). Atherosclerotic lesion areas are quantified in (B) and (D). Immunofluorescent staining of MOMA-2 (green) and DAPI (blue) identifying monocytes/macrophages in aortic root sections (E). Immunofluorescence highlighting smooth muscle cells (SMCs) by staining for α-SMA (green) and DAPI (blue) in aortic root sections; lesional SMCs were quantified in (F). Images are representative of 9 mice/Vim group and 7 mice/PBS group. Values are expressed as the mean ± SD. Statistical analyses were performed using a *t*-test.

Moreover, vimentin is secreted by endothelial cells and activated macrophages throughout the body [8,9], with phosphorylation of this protein occurring in its secretory process [8,9,24]. Extracellular vimentin secreted by macrophage is involved in two important functions of activated macrophages, the generation of oxidative metabolites and killing bacteria [9]. Serological levels of citrullinated vimentin in patients with rheumatoid arthritis are increased relative to healthy patients, and therefore, citrullinated vimentin is detected as an early pathological marker for this autoimmune disease [25]. These data indicate that extracellular vimentin is probably related to immune function. The pro-inflammatory cytokine TNF-α and LPS induce vimentin secretion, whereas the anti-inflammatory cytokine IL-10 blocks vimentin secretion [9,26], suggesting also that secretory vimentin is involved in the inflammatory response. A recent study suggested that vimentin deficiency in macrophages could attenuate atherosclerosis in *Ldlr*$^{-/-}$ mice [27], but the atherogenic effect of secretory vimentin is not clear. Our study has shown the association of increased secretory vimentin levels with CAD in patients and vimentin protein-induced promotion of inflammation and atherogenesis *in vitro* and *in vivo*. These results, for the first time, directly link increased production of secretory vimentin to inflammation and atherosclerosis.

We recognize that a major limitation in our patient study is its cross-sectional nature, which allow us to detect associations of serum secretory vimentin levels with CAD but not to formulate risk predictions. We also acknowledge that more studies are needed to clarify the functions of vimentin. For instance, what is the physiological role and modulation of cleaved and secretory vimentin; what is the relationship among cleaved vimentin, secretory vimentin and intracellular vimentin; and does inhibiting secretory vimentin production lead to plaque regression or prevent further progression of established atherosclerosis. Last, it would be more meaningful if we test the inflammatory and atherogenic effects of secretory vimentin using mice with a secretory vimentin deficiency or low circulatory vimentin levels. These questions will be addressed in future studies.

6. Conclusions

The present study demonstrates that serum secretory vimentin levels are closely related to the presence and severity of CAD in patients. Vimentin also promotes atherogenesis in mice.

Acknowledgement

We gratefully acknowledge the participation of all the study subjects. In particular, we thank Yang Dai for providing technical assistance, Lin Lu for assisting with statistical analysis, and Feng Hua Ding for assisting with manuscript preparation.

Authors contributions

Dong Huo Gong, Shuai Chen, Ying Shen, Lin Jun Yu, Li Li Liu, Qiu Jing Chen and Jing Liu performed experiments; Yang Dai, Xiao Xiang Yan, Ying Shen, Zhen Kun Yang, Jian Hu and Xiao Qun Wang interpreted results of experiments and prepared figures; Rui Yan Zhang and Wei Feng Shen analysed data; Feng Hua Ding and Lin Lu drafted manuscript and approved final version of manuscript.

Source of funding

This study was supported by National Natural Science Foundation of China (81470469, 81770447, 81670451, 81770430, 81770437), Shanghai Science and Technology Committee (15411963700) and Shanghai Municipal Education Commission-Gaofeng Clinical Medicine Grant Support (20181801), Shanghai Rising-Star Program (17QA1403000), and Shanghai Municipal Commission of Health and Family Planning Foundation (2018YQ17).

Conflict of interest

None.

Appendix A. Supplementary data

Supplementary data to this article can be found online at https://doi.org/10.1016/j.ijcard.2019.02.032.

References

[1] P. Libby, Inflammation in atherosclerosis, Arterioscler. Thromb. Vasc. Biol. 32 (2012) 2045–2051.
[2] J.M. Dave, K.J. Bayless, Vimentin as an integral regulator of cell adhesion and endothelial sprouting, Microcirculation 21 (2014) 333.
[3] T. Lang, J.P.W. Lee, K. Elgass, et al., Macrophage migration inhibitory factor is required for NLRP3 inflammasone activation, Nat. Commun. 9 (2018) 2223.
[4] G. Dos Santos, M.R. Rogel, M.A. Baker, et al., Vimentin regulates activation of the NLRP3 inflammasone, Nat. Commun. 6 (2015) 6574.
[5] M. Nieminen, T. Henttinen, M. Merinen, F. Marttila-Ichihara, J.E. Eriksson, S. Jalkanen, Vimentin function in lymphocyte adhesion and transcellular migration, Nat. Cell Biol. 8 (2006) 156–162.
[6] S. Samanta, K. Anderson, S. Moran, D. Hawke, D. Gorenstein, M. Fornage, Characterization of a human 12/15-lipoxygenas promoter variant associated with atherosclerosis identifies vimentin as a promoter binding protein, PLoS ONE 7 (2012), e42417.
[7] Y. Huo, L. Zhao, M.C. Hyman, et al., Critical role of macrophage 12/15-lipoxygenase for atherosclerosis in apolipoprotein E-deficient mice, Circulation 110 (2004) 2024–2031.
[8] B. Xu, R.M. deWaal, N. Mor-Vaknin, C. Hibbard, D.M. Markovitz, M.L. Kahn, The endothelial cell-specific antibody PAL-E identifies a secreted form of vimentin in the blood vasculature, Mol. Cell. Biol. 24 (2004) 9198–9206.
[9] N. Mor-Vaknin, A. Punturieri, K. Sitwala, D.M. Markovitz, Vimentin is secreted by activated macrophages, Nat. Cell Biol. 5 (2003) 59–63.
[10] Y. Dai, Y. Shen, Q.R. Li, et al., Glycated apolipoprotein A-IV induces atherogenesis in patients with CAD in type 2 diabetes, J. Am. Coll. Cardiol. 70 (2017) 2006–2019.
[11] G.G. Gensini, A more meaningful scoring system for determining the severity of coronary heart disease, Am. J. Cardiol. 51 (1983) 606.
[12] L. Lu, R.Y. Zhang, X.Q. Wang, et al., C1q/TNF-related protein-1: an adipokine marking and promoting atherosclerosis, Eur. Heart J. 37 (2016) 1762–1771.
[13] L. Lu, Y.N. Wang, M.C. Li, et al., Reduced serum levels of vasostatin-2, an anti-inflammatory peptide derived from chromogranin A, are associated with the presence and severity of coronary artery disease, Eur. Heart J. 33 (2012) 2297–2306.
[14] M.J. Pencina, R.B. D'Agostino Sr., R.B. D'Agostino Jr., R.S. Vasan, Evaluating the addedr predictive ability of a new marker: from area under the ROC curve to reclassificatio and beyond, Stat. Med. 27 (2008) 157–172.
[15] P.M. Ridker, N.P. Paynter, N. Rifai, J.M. Gaziano, N.R. Cook, C-reactive protein and parental history improve global cardiovascular risk prediction: the Reynolds Risk Score for men, Circulation 118 (2008) 2243–2251.
[16] M. Nieminen, T. Henttinen, M. Merinen, et al., Vimentin function in lymphocyte adhesion and trascellular migration, Nat. Cell. Biol. 8 (2) (2006) 156–162.
[17] F. Danielsson, M.K. Peterson, H. Caldeira Araujo, F. Lautenschlager, A.K.B. Gad, Vimentin diversity in health and disease, Cells 7 (2018), piiE147.
[18] M.I. Rodriguez, A. Peralta-Leal, F. O-Valle, et al., PARP regulates metastatic through modulation of vimentin-induced malignant transformation, PLoS Genet. 9 (6) (2013) e1003531.
[19] F. Cheng, Y. Shen, P. Mohanasundaram, et al., Vimentin coordinates fibroblast proliferation and keratinocyte differentiation in wound healing via TGF-B-Slug signaling, Proc. Natl. Acad. Sci. U. S. A. 113 (30) (2016) E4320–E4327.
[20] C.L. Hyder, K.O. Isoniemi, E.S. Torvaldson, et al., Insights into intermediate filament regulation from development to ageing, J. Cell. Sci 124 (2011) 1363–1372.
[21] H.S. Xiao, Q. Xie, J.Y. Zhong, et al., Effect of vimentin on activation of NLRP3 inflammasome in the brain of mice with EV71 infection, Nan Fang Yi Ke Da Xue Xue Bao 38 (6) (2018) 704–710.
[22] J. Ivaska, H.M. Pallari, J. Nevo, J.E. Eriksson, Novel functions of vimentin in cell adhesion, migration, and signaling, Exp. Cell Res. 313 (2007) 2050–2062.
[23] C. Margadant, A. Sonnenberg, Integrin-TGF-beta crosstalk in fibrosis, cancer and wound healing, EMBO Rep. 11 (2010) 97–105.
[24] K. Lee, L. Liu, Y. Jin, S. Fu, J.L. Rosales, Cdk5 mediates vimentin ser56 phosphorylation during GTP-induced secretion by neutrophils, J. Cell. Physiol. 227 (2012) 739–750.
[25] H. Poulsom, P.J. Charles, Antibodies to citrullinated vimentin are a specific and sensitive marker for the diagnosis of rheumatoid arthritis, Clin. Rev. Allergy Immunol. 34 (2008) 4–10.
[26] S.J. Lee, J.D. Yoo, S.Y. Choi, O. Kwon, The expression and secretion of vimentin in the progression of non-alcoholic steatohepatitis, BMB Rep. 47 (2014) 457–462.
[27] H. Liliana, P.S. Jeanna, M. Adil, et al., Vimentin deficiency in macrophages induces increased oxidative stress and vascular inflammation but attenuates atherosclerosis in mice, Sci. Rep. 8 (2018), 16973.